Published in final edited form as:
Toxicol Appl Pharmacol. 2014 June 1; 277(2): 200–209. doi:10.1016/j.taap.2014.03.021.

Environmentally Persistent Free Radicals Inhibit Cytochromes P450 Activity in Rat Liver Microsomes

James R. Reed[*,‡], **George F. Cawley**[*], **Taylor G. Ardoin**[*], **Barry Dellinger**[†], **Slawomir M. Lomnicki**[†], **Farhana Hasan**[†], **Lucy W. Kiruri**[†], and **Wayne L. Backes**[*]

[*]Department of Pharmacology and Experimental Therapeutics, and The Stanley S. Scott Cancer Center, Louisiana State University Health Science Center, 533 Bolivar St., New Orleans, LA 70112, USA

[†]Department of Chemistry, Louisiana State University, Baton Rouge, LA, 70803, USA

Abstract

Combustion processes generate particulate matter that affects human health. When incineration fuels include components that are highly enriched in aromatic hydrocarbons (especially halogenated varieties) and redox-active metals, ultrafine particulate matter containing air-stable, environmentally persistent free radicals (EPFRs) are generated. The exposure to fine EPFRs (less than 2.5 μm in diameter) has been shown to negatively influence pulmonary and cardiovascular functions in living organisms. The goal of this study was to determine if these EPFRs have a direct affect on cytochrome P450 function. This was accomplished by direct addition of the EPFRs to rat liver microsomal preparations and measurement of several P450 activities using form-selective substrates. The EPFRs used in this study were formed by heating vapors from an organic compound (either monochlorophenol (MCP230) or 1,2- dichlorobenzene (DCB230)) and 5% copper oxide supported on silica (approximately 0.2 μm in diameter) to 230°C under vacuum. Both types of EPFRs (but not silica, physisorbed silica, or silica impregnated with copper oxide) dramatically inhibited the activities of CYP1A, CYP2B, CYP2E1, CYP2D2 and CYP3A when incubated at concentrations less than 0.1 mg/ml with microsomes and NADPH. Interestingly, at the same concentrations, the EPFRs did not inhibit HO-1 activity or the reduction of cytochrome c by NADPH-cytochrome P450 reductase. CYP2D2-selective metabolism by rat liver microsomes was examined in more detail. The inhibition of CYP2D2-selective metabolism by both DCB230- and MCP230-EPFRs appeared to be largely noncompetitive and was attenuated in the presence of catalase suggesting that reactive oxygen species may be involved in the mechanism of inhibition.

Keywords

cytochrome P450; metabolism; inhibition; nanoparticle; radical

[‡]Author to whom correspondence should be addressed. rreed@lsuhsc.edu; phone: (504) 568-5699; fax: (504) 568-2361.

Introduction

Fine (< 2.5 μm in diameter) and ultrafine (< 0.1 μM) particulate matter are environmentally pervasive types of pollutants that arise predominantly from combustion processes (Cass *et al.*, 2000; Kennedy, 2007; Oberdorster *et al.*, 2005). These types of particulate matter are capable of deeply penetrating the lower airways and alveoli of lungs and can be taken up into circulation from the lungs and distributed systemically (Kreyling *et al.*, 2009; Nemmar *et al.*, 2001; Nemmar *et al.*, 2002). Epidemiologic evidence suggests that exposure to fine and ultrafine particulate matter is related to an increase in cardiac morbidity and mortality (Brook *et al.*, 2010; Dockery, 2001). Furthermore, exposure to these types of particulate matter has been correlated with impaired lung development and function in children (Gauderman *et al.*, 2004) and exacerbation of pulmonary diseases such as chronic obstructive pulmonary disease (Pope, III *et al.*, 2002), asthma (Maestrelli *et al.*, 2011), and lower tract respiratory infections (Hwang *et al.*, 2002).

It is generally believed that the adverse health effects of fine and ultrafine particulate matter are caused by an inflammatory response to particulate matter-related oxidative stress (Cormier *et al.*, 2006). The particulate matter derived from combustion contain a complex mixture of particulate matter, organic compounds (including aromatics and halogenated species), and metals. It has been demonstrated that combustion leads to chemisorption of the organic compounds to metal oxide clusters existing on the surface of the nanoparticles (Lomnicki *et al.*, 2003; Lomnicki *et al.*, 2008). In the process, an electron is transferred from the organic to the metal oxide to create resonance-stabilized semiquinone and phenoxyl type radicals on the surface of the nanoparticle (Lomnicki *et al.*, 2008). Such particle-radical systems, referred to as environmentally persistent free radicals (EPFRs), are relatively air-stable (lasting for days or even weeks) and are capable of redox cycling in biological systems. It has been shown that the EPFRs lead to the generation of superoxide, hydrogen peroxide and the highly destructive hydroxyl radical when suspended in solution (Khachatryan *et al.*, 2011). Because of the stability of EPFRs, it has been postulated that their deleterious effects are caused by prolonged oxidation/reduction activities in living systems (Dellinger *et al.*, 2001).

The chemistry and reactivity of EPFR model systems composed of 5% (w/w) of CuO supported on silica (< 0.2 μm in diameter), with chemisorbed aromatic halocarbon (either 1,2-dichlorobenzene (DCB230) or 2-monochlorophenol (MCP230)) have been studied extensively (Balakrishna *et al.*, 2009; Lomnicki *et al.*, 2008). Because these EPFRs have a defined composition, their effects on living systems can be more easily interpreted than those of EPFRs that are derived from the complex mixture of components found in particulate matter sampled from real-life combustion sites. The effects of these model EPFRs in living systems has now been studied by several labs to characterize the cardiovascular and pulmonary damage caused by EPFRs (Balakrishna *et al.*, 2011; Lord *et al.*, 2011; Mahne *et al.*, 2012).

The cytochromes P450 (P450 or CYP) constitute a gene superfamily of enzymes that are variably expressed in tissues from virtually all plants and animals (Nelson, 2003). The mammalian, drug-metabolizing varieties of these enzymes use molecular oxygen and

electrons transferred from a separate redox partner, NADPH-cytochrome P450 reductase (CPR) or both CPR and cytochrome b_5, to catalyze the mixed function oxidation of both endogenous and xenobiotic compounds (Loida *et al.*, 1993; White *et al.*, 1980). In addition to making hydrophobic, exogenous compounds more hydrophilic and easier to eliminate from the body, P450s have been shown to bioactivate many chemicals to electrophilic products that cause cellular damage by binding to nucleic acid, membranes, and proteins (Guengerich, 2001). Exposure to particulate matter from diesel exhaust has been shown to modulate the expression and activities of P450 enzymes (Hatanaka *et al.*, 2001; Rengasamy *et al.*, 2003). It is not clear what roles P450 activities play in modulating the adverse health effects of particulate matter.

In this study, we determined the effects of the model EPFRs (MCP230 and DCB230 (Lomnicki *et al.*, 2008)) on P450 activities in rat liver microsomes. By using the tandem approach of chemical induction to over-express specific forms of P450 and probe substrates that have shown to be selectively metabolized by individual P450 enzymes in rat liver, we have found that the EPFRs generally inhibited metabolism by six different forms of P450 (all of the P450 forms tested). In addition, the inhibition of one of the forms of P450, CYP2D2-related activity was characterized in more detail. Surprisingly, EPFRs did not inhibit the NADPH-dependent reduction of cytochrome c by CPR in rat liver microsomes or heme degradation catalyzed by HO-1 in liver microsomes from cadmium-induced rats. Finally, the role of reactive oxygen species generation was considered in the mechanism of P450 inhibition by the EPFRs.

Methods

Chemicals

The reagents used were of the highest commercial quality available. Pyrazole, β-naphthoflavone (BNF), α-naphthoflavone (ANF), cadmium chloride, methanol, clotrimazole, orphenadrine, *p*-nitrophenol (PNP), chlorzoxazone, quinine, 7-methoxyresorufin (MRF), 7-hydroxycoumarin, 7-benzyloxyquinoline (BQ), 7-pentoxyresorufin (PRF), resorufin, phenobarbital, and sulfaphenazole were purchased from Sigma-Aldrich (St. Louis, MO). The P450 substrates and inhibitors, 3-cyano-7-ethoxycoumarin (CEC); 3-[2-(N,N-diethyl-N-methylammonium)ethyl]-7-methoxy-4-methylcoumarin (AMMC), 7-hydroxyquinoline, 3-cyano-7-hydroxycoumarin (CHC), and 3-[2-(diethylamino)ethyl]-7-hydroxy-4-methylcoumarin hydrochloride (AHMC) were purchased from BD Gentest (Woburn, MA).

Treatment of rats

Male Sprague Dawley rats (five rats/group) were dosed by intraperitoneal injection. The animals were euthanized 24 hr after the last dose. Treatment groups consisted of the following: 1) 0.9% saline control; 2) 80 mg/kg phenobarbital (injected from an 80 mg/ml saline solution for three successive days); 3) 200 mg/kg pyrazole (injected from a 200 mg/ml saline solution for three successive days); 4) corn oil control; 5) 40 mg/kg BNF as a 1% solution in corn oil (one day treatment); and 6) 4.57 mg/kg cadmium chloride (injected from a 4.75 mg/ml saline solution for one day only). All animal protocols were prepared in

accordance with the Guide for the Care and Use of Laboratory Animals and approved by the LSUHSC Institutional Animal Care and Use Committee.

Preparation of microsomes and western blotting

Livers were excised immediately after the rats were euthanized. Microsomes and rat liver cytosols were prepared by differential centrifugation and protein concentrations were determined as described previously (Cawley *et al.*, 2001). The microsomes from each rat were diluted to 20 mg/ml protein in 10 mM potassium phosphate (pH 7.4) and stored at −80°C. The microsomes from each treatment group were pooled by taking equal volumes of microsomes from each animal before using as a source of enzymes for enzymatic assays and western blot analysis. Electrophoresis was run with a 10% polyacrylamide gel by loading 40 μg of each pooled set of microsomes in separate lanes with the exception of the gel used to blot for HO-1. This gel was loaded with 100 μg of microsomes from all of the treatment groups except the cadmium chloride group, and the pooled microsomes from cadmium chloride-treated animals were loaded at 40 μg. Electrophoresis was run at 200 V for 50 min, and the protein was transferred to nitrocellulose membranes by running for 1 hour at 100 V. Western blotting was performed by incubating with primary antibodies for 2 hr at room temperature. All P450 antibodies were tested for specificity by screening their ability to react with purified rabbit CYP1A2, CYP2B4, and CYP2E1 and with human CYP3A4. The antibodies used only interacted with the intended form of P450 and did not cross-react with the other P450 forms, based on our studies and those reported by the suppliers. The primary antibodies used in this study are as follows: CYP1A2 (Abcam (Cambridge, MS) cat #: ab4227 at 1:4000), CYP2B1 (Oxford Biomedical Research (Rochester Hills, MI) cat #: PM25 at 1:1000), CYP2E1 (Oxford Biomedical Research cat #: PM32 at 1:1000); CYP3A1 (Oxford Biomedical Research cat #: PM40 at 1:1000), and HO-1 (US Biologics (Swampscott, MS) cat #: H1847-69D at 1:200). After washing, the membranes were incubated with secondary antibody conjugated to horseradish peroxidase, and the blots were developed by chemiluminescence using SuperSignal West Pico substrate (Thermo Scientific, Rockford, IL).

Preparation of model EPFRs

Particles (~ 0.2 μm in diameter) containing 5% copper oxide (w/w) supported on CAB-O-SIL EH-5 fumed silica (Cabot Corporation, Billerica, MA) with and without inclusion of either 1,2-dichlorobenzene-born radical or 2-monochlorophenol-born radical were prepared as described previously (Balakrishna *et al.*, 2009; Lomnicki *et al.*, 2008). Briefly, silica was first impregnated with copper nitrate hemipentahydrate by incubation in a 0.1 M solution for 24 hours at room temperature. The impregnated silica was then dried at 120°C for 12 hours and subsequently heated for 5 hours in air at 450°C to complete the calcination process. The prepared particles were placed in vacuum ($<10^{-2}$ torr) and heated to 230°C before being dosed with vapors of the organic constituents at 10 torr in a custom-made vacuum exposure chamber for 5 min. These conditions are representative to those that occur in the post-flame, cool-down zone during the combustion process (Cormier *et al.*, 2006). The samples were cooled to room temperature and evacuated for 1 hr (10^{-2} torr). The radical contents of the EPFRs were analyzed by electron paramagnetic resonance spectroscopy (EPR) as described previously (Khachatryan *et al.*, 2011), and the samples were then weighed in 15 mg portions

and sealed in ampoules under vacuum. The concentration of radicals on particles was expressed in spins/g, representing number of radicals per unit mass of the sample. Samples were used for the experiments reported within two to three weeks after synthesis. Pure silica substrate, the silica containing 5% copper oxide, and silica exposed to vapors of MCP and DCB at 50°C (physisorbed MCP100 and DCB100, respectively) were used as controls (as indicated in the results).

Suspension of particle

To prepare the silica for the in vitro incubations with microsomal protein, it was resuspended at a concentration of 2 mg/ml in a solution that contained 0.9% (w/v) sodium chloride and 0.02% (v/v) Tween 80. The solution was adjusted to the pH range 7.0 to 7.5 with 1% sodium bicarbonate before adding to the particles. After addition of the saline/Tween 80 solution, the samples were vortexed vigorously for 1 minute and then probe-sonicated, with a sonic dismembrator, model 100 (Fisher Scientific, Pittsburgh, PA) on ice (at 10–14 watts) for four 30-second intervals with 30 seconds between each sonication cycle. The particles (silica, silica with 5% copper oxide, physisorbed silica, or EPFRs) were vigorously vortexed immediately before adding to the incubations with protein (final concentrations indicated in the results). When conditions were compared, all of the incubations contained the same volume of the saline/Tween 80 solution that was used to suspend the particles.

Assays to measure activities that were selective for individual P450 enzymes

With the exception of the assay to measure the CYP2E1-selective conversion of PNP to *p*-nitrocatechol, the P450-selective assays were performed in 0.1 ml volumes in a 96-well plate using a buffer that contained 0.05 M HEPES (pH 7.5) and 15 mM $MgCl_2$. Each assay also contained 0.5 mg/ml of microsomal protein from treated rats as indicated in the Results. The PNP assay to measure CYP2E1 activity used pyrazole microsomes at 1 mg/ml and a buffer containing 0.05 M potassium phosphate (pH 6.8) and 15 mM $MgCl_2$. All reactions were performed at 37°C and were started by adding NADPH at a final concentration of 0.4 mM. All assays were performed by monitoring real-time fluorescence or absorbance changes (as indicated) with a SpectraMax M5 plate reader (Molecular Devices, Sunnyvale, CA). Unless indicated otherwise, all substrate and inhibitor stock solutions were prepared in methanol and were diluted 100-fold when added to the assay mixtures. To increase the specificities of the different P450 reactions, the substrates were either incubated at or below the K_m concentrations reported for the rat P450s or at concentrations which had been shown to be selective for rat forms of P450. Similarly, selective inhibitors for the rat isoforms were tested at concentrations reported to be effective in the literature (as indicated below). The references cited in the following paragraphs in association with the probe substrates and inhibitors are those that validate the specificity of these compounds for the rat forms of P450.

The assay for rat CYP1A1 used 40 μM CEC (Stresser *et al.*, 2002) which, because of solubility limits, was diluted 1:50 from a 2 mM methanolic solution. The assay for CYP1A2 used 4 μM MRF (Liu *et al.*, 2004; Nerurkar *et al.*, 1993). In related experiments, we have found that rabbit CYP2E1 also is able to metabolize this substrate (data not shown).

Therefore, the CYP1A2 incubations of MRF dealkylation included 500 μM chlorzoxazone to inhibit CYP2E1-dependent MRF metabolism. Higher concentrations of chlorzoxazone (1 mM) appeared to affect CYP1A activities as this concentration inhibited the rate of MRF metabolism by BNF-induced microsomes by approximately 35% (data not shown). The activities of CYP1A1 and CYP1A2 were measured in real time by monitoring fluorescence to determine the rates of formation of CHC (Ex: 390 nm; Em: 460 nm) and resorufin (Ex: 535 nm; Em: 585 nm), respectively. The amounts of the products formed were determined by comparison to standard curves of the compounds. Both CYP1A1 and CYP1A2 activities were measured using microsomes from BNF-treated rats and were inhibited by using 10 μM ANF as reported previously (Burke *et al.*, 1977; Wiebel *et al.*, 1971).

The assay for rat CYP2B-related activity was measured with microsomes from phenobarbital-treated animals and used 5 μM PRF (Burke *et al.*, 1994), and the rate of product formation was determined by monitoring fluorescence (Ex. 535 nm; Em: 585) and referring to a resorufin standard curve. The activity of CYP2B was inhibited using 40 μM orphenadrine as reported previously (Reidy *et al.*, 1989).

The assay for rat CYP2E1 activity was measured with microsomes from pyrazole-treated rats and used 100 μM PNP (Koop *et al.*, 1989) and the kinetic assay of Allis and Robinson (Allis *et al.*, 1994). The rate of change in absorbance at 480 nm was used to determine the rate of the reaction by using the extinction coefficient for *p*-nitrocatechol at this wavelength ($3.57\ mM^{-1}cm^{-1}$ (Allis *et al.*, 1994)). One important modification of the published assay was to omit the NADPH generating system from the reaction. Although the authors claimed the rates were higher with the NADPH generating system, we found that the 480 nm absorbance increased linearly with time in control reactions with the glucose-6-phosphate regenerating system that were initiated with NADPH in the absence of microsomes or PNP. Rat CYP2E1 activity was inhibited by 500 μM chlorzoxazone as reported previously (Howard *et al.*, 2001).

AMMC has been demonstrated to be a specific probe substrate for metabolism by CYP2D2 (Makaji *et al.*, 2010; Stresser *et al.*, 2002). The assay for rat CYP2D2-related activity used AMMC at 20 μM, and the rate of metabolism was determined by monitoring the rate of change in fluorescence with time (Ex: 390 nm; EM: 460 nm) and referring to an AHMC standard curve. The activity by rat CYP2D2 was inhibited by 1 μM quinine as reported previously (Barham *et al.*, 1994; Makaji *et al.*, 2010). Because the AMMC assay is relatively specific for CYP2D2-related activity, the kinetic constants for metabolism of this substrate by rat liver microsomes from saline-treated rats were determined in the presence and absence of EPFRs by measuring metabolism over the range of AMMC concentrations indicated in the results. The K_m and V_{max} values were determined by fitting the data using a nonlinear regression analysis with the Michaelis Menten equation (Prism 5.02, GraphPad, La Jolla, CA). The inhibition by the two types of EPFRs (MCP230 & DCB230) was characterized by analyzing double reciprocal plots of the data as indicated in the results.

The assay for rat CYP3A-related activity used 100 μM BQ (Makaji *et al.*, 2010; Renwick *et al.*, 2001; Stresser *et al.*, 2002), and the rate of metabolism was determined by monitoring the change in fluorescence (Ex: 409; Em: 530) and referring to a 7-hydroxyquinoline

standard curve. Because other P450 forms have been shown to metabolize this substrate in rats (Stresser *et al.*, 2002), the incubations also included 1 μM quinine, 40 μM orphenadrine, and 10 μM ANF to inhibit metabolism from CYP2D, CYP2B, and CYP1A, respectively. Rat CYP3A activity was inhibited by 0.1 μM clotrimazole as reported previously (Turan *et al.*, 2001).

Other assays

Rat HO-1 activity in liver microsomes from cadmium-induced rat was measured as described previously (Reed *et al.*, 2011) in 0.1 M HEPES buffer (pH 7.4) containing 0.5 units/μL catalase; 15 μM hemin (added from a 2.5 mM stock that was prepared by first, using bath-sonication to dissolve hemin in a 0.1 M potassium hydroxide solution at a concentration of 12.5 mM and then diluting to the final stock concentration with 0.1 M HEPES (pH 7.4)); 1.0 mg/ml rat liver microsomes; and a 1:7 dilution of rat liver cytosol. The 0.1 ml reactions were initiated with 0.01 ml of 4 mM NADPH, and the rate of heme degradation at 37°C was determined by measuring the real-time rate of change in the absorbance difference between 464 nm and 530 nm (ε= 0.04 mM^{-1} cm^{-1}) caused by the formation of bilirubin (Maines, 1996).

The NADPH-dependent reduction of cytochrome c by liver microsomes from uninduced rats was measured in a 0.1 M potassium phosphate buffer (pH 7.7) containing 0.65 mg/ml cytochrome c and 0.25 mg/ml microsomes. The 0.1 ml reactions at 37°C were initiated with 0.01 ml of 4 mM NADPH, and the reduction of cytochrome c was monitored in real time by measuring the absorbance at 548 nm. The rate of the reaction was determined from the difference extinction coefficient for the reduced and oxidized forms of reduced cytochrome c (0.021 $mM^{-1}cm^{-1}$) (Phillips *et al.*, 1962).

Results

Characterization of P450-specific metabolism by rat liver microsomes

Differential chemical induction of rats was used to amplify specific forms of P450s in liver microsomes. This type of approach has been used successfully to improve the P450-specificity of the metabolism of probe substrates (Burke *et al.*, 1985){Renwick, 2001 2727/id; Wiebel, 1971 2735/id; Nerurkar, 1993 2717/id}. It has been shown that the specificities of P450 probe substrates can be vastly improved if the P450 of interest is induced in the microsomes (Burke *et al.*, 1994). Figure 1 shows a comparison of five western blots for each of the inducible enzymes in the pooled rat liver microsomes from the treated animals that were used in this study. Figure 1 shows that the chemical treatments dramatically increased expression of the desired enzymes. CYP2D2 is constitutively expressed and is not known to be inducible. Thus, a western blot was not performed for this enzyme and microsomes from saline-treated rats were used to measure metabolism of its probe substrate, AMMC. Consistent with the specificity of AMMC for CYP2D2, 100% of the metabolism of this substrate by liver microsomes from saline-treated rats was inhibited by 1 μM of the CYP2D-specific inhibitor, quinine (Table 1).

BNF was used to induce CYP1A P450 enzymes. Densitometric analysis of the western blots indicated that CYP1A expression (Figure 1, row 1) was increased over 15-fold in rat liver, relative to corn oil treated animals, following treatment with BNF (lane 4). As a result, CYP1A activity was assessed by using the microsomes from BNF-treated animals, and CYP1A1 activity was measured using CEC at a concentration of 40 μM. Metabolism under these conditions was shown to be very selective for this form of P450 relative to that by CYP1A2 and other forms of rat P450 (Stresser *et al.*, 2002). Although CYP1A2 also is able to metabolize CEC, the high rate of metabolism of this substrate by the microsomes from BNF-induced rats (Table 2) is consistent with the high turnover rate of rat CYP1A1 for this substrate (relative to that of CYP1A2) and supports the use of CEC as a probe substrate for CYP1A1. Table 1 shows that 95% of the metabolism of CEC by BNF-treated microsomes was inhibited by the CYP1A-specific inhibitor, ANF. Conversely, rat liver microsomal metabolism of 5 μM MRF has been shown to be a specifically catalyzed by CYP1A2 relative to that by CYP1A1 (Nerurkar *et al.*, 1993). Approximately 98% of this activity was inhibited by the CYP1A-specific inhibitor, ANF, at a concentration of 10 μM (Table 1). Thus, CEC and MRF metabolism by microsomes from BNF-treated animals were used as specific probes for CYP1A1 and CYP1A2, respectively.

CYP2B enzymes are expressed at very low levels in livers from control rats but are induced dramatically by treatment of the animals with phenobarbital. Figure 1 shows the induction caused by phenobarbital treatment (row 2, lane 2). The immunoreactive band corresponding to CYP2B1 was not visible in the microsomes from rats that were not treated with phenobarbital, and densitometric analysis of the western blot showed that the level of protein was dramatically increased relative to the level in liver microsomes from saline-treated animals. PRF has been shown to be a very selective substrate for CYP2B enzymes in rat (Burke *et al.*, 1994; Nerurkar *et al.*, 1993). Table 1 shows that 91% of the metabolism of 5 μM PRF by PB-microsomes was inhibited by the CYP2B-selective inhibitor, orphenadrine at 40 μM.

CYP2E1 was expressed in rat liver following all conditions of treatment. The enzyme is induced upon treatment with many of the small molecular weight, organic compounds that are also substrates for CYP2E1 (Koop *et al.*, 1985; Koop *et al.*, 1990). Treatment of rats with pyrazole induced CYP2E1 expression approximately 5-fold relative to treatment with saline solution (row 3, Figure 1). PNP has been used as a CYP2E1-specific substrate. In our hands, metabolism of 100 μM PNP by liver microsomes from pyrazole-treated rats was inhibited by 73% with 500 μM chlorzoxazone, a CYP2E1-sepcific inhibitor of rat CYP2E1. This concentration of chlorzoxazone was roughly twice the K_m of rat CYP2E1 for this compound, when studied as a substrate (Howard *et al.*, 2001). Thus, the level of inhibition is approximately what would be expected if the activity was solely attributable to metabolism by CYP2E1, and the data were supportive of using these conditions as a probe reaction to monitor CYP2E1-mediated activity.

CYP3A enzymes are constitutively expressed in rat liver. However, induction by treatment with phenobarbital resulted in a 5.5-fold increase in CYP3A expression relative to that in microsomes from saline-treated rats (Figure 1, row 4). Metabolism of the substrate, BQ, at a concentration above 25 μM, was a relatively specific assay for CYP3A activity when

compared to its metabolism by other rat P450 forms (Renwick *et al.*, 2001; Stresser *et al.*, 2002). However, it was suggested that metabolism by CYP1A, CYP2D, and CYP2B could possibly contribute to the total BQ metabolism by rat liver microsomes (Stresser *et al.*, 2002). As a result, we examined the effects of specific inhibitors for these P450s on metabolism of 40 μM BQ by liver microsomes from various treatment groups. To assess the potential for metabolism of BQ by CYP2B enzymes, we measured the inhibition of BQ metabolism by the CYP2B-specific inhibitor, orphenadrine. When tested at a concentration that inhibited over 90% of the metabolism of the CYP2B-specific substrate, PRF (Table 1), 40 μM orphenadrine inhibited only 27% of total BQ metabolism by microsomes from phenobarbital-treated rats. Similarly, 10 μM ANF inhibited less than 10% of BQ metabolism by microsomes from BNF-treated rats. In addition, the CYP2D-specific inhibitor, quinine, inhibited less than 15% of BQ metabolism by microsomes from saline-treated animals at a concentration of 1 μM (a concentration which completely inhibited the metabolism of the CYP2D2 probe, AMMC). Conversely, the CYP3A-specific inhibitor, clotrimazole, when used at a concentration of 0.1 μM, inhibited over 85% of BQ metabolism by microsomes from phenobarbital-treated animals and over 90% of metabolism by microsomes from saline-treated rats. Furthermore, this concentration of clotrimazole had no significant effects on the rates of metabolism of MRF and AMMC by rat liver microsomes and only inhibited the microsomal-mediated rate of metabolism of PRF by 20% (data not shown). Thus, in agreement with previous findings (Renwick *et al.*, 2001), BQ is metabolized predominantly by CYP3A in rat liver microsomes and was used as a substrate probe to measure activity by CYP3A in liver microsomes from phenobarbital-treated animals. To increase the specificity of the reaction by CYP3A in microsomes from phenobarbital-treated animals, the reactions were performed in the presence of 10 μM ANF, 1 μM quinine, and 40 μM orphenadrine.

Effects of Particles on metabolism by rat liver P450s

Metabolism of the selected probe substrates by rat liver microsomes was measured in the presence and absence of 0.05 mg/ml particles. The rates of metabolism by all of the P450s were markedly inhibited in the presence of 0.05 mg/ml EPFRs but not in the presence of fumed silica (Table 2). Specific metabolism by CYP1A1, CYP1A2, CYP2B, and CYP2E1 were all inhibited by 85% or greater by the two types of EPFRs. Typically, slightly higher amounts of inhibition were observed with MCP230 relative to DCB230. The one exception to this trend was observed with the CYP2E1-mediated metabolism of PNP which was more strongly inhibited by DCB230. The rates of the CYP2D2- and CYP3A-mediated reactions were less inhibited by the EPFRs. DCB230 and MCP230 inhibited the CYP2D2-mediated metabolism of AMMC by 68% and 80% and the CYP3A-mediated metabolism of BQ by 52% and 73%, respectively.

The effects of the EPFRs on P450-mediated activity were dose- and EPFR-dependent as shown in Figure 2. This figure shows the rates of AMMC metabolism by liver microsomes from saline-treated rats as a function of EPFR concentration. Because of slight batch to batch variability in the potency of the EPFRs, the levels of inhibition are slightly less than those reported in Table 2. With this in mind, it should be emphasized that the data for Table 2 and Figures 6 and 7 were collected using the same batch of EPFRs. Thus, we believe the relative potencies of the EPFRs to inhibit different P450 activities are accurately depicted by

the data. Figure 2 shows that the level of inhibition of metabolism of AMMC by rat liver microsomes varied with the concentration of the EPFRs, and the activity by both EPFRs was significantly inhibited at 0.025 mg/ml, and completely inhibited at about 0.1 mg/ml.

Inhibition of P450 activities by non-EPFR particles

Dose-dependent inhibition of AMMC metabolism by the copper oxide-containing silica, which was used as a control, was not observed until the particle concentration exceeded 0.1 mg/ml, and the reaction was almost entirely inhibited when the particle concentration reached 0.825 mg/ml (Figure 2). The effects of the other non-EPFR particles (silica, copper oxide-containing silica, physisorbed DCB100, and physisorbed MCP100) on the P450-mediated metabolism of all of the probe substrates were assessed at a particle concentration of 0.2 mg/ml (Table 3), a concentration where we obtained complete inhibition by the EPFRs. In general, the highest levels of inhibition were observed when the reactions were incubated with the copper oxide-containing silica, and there were either no significant or only moderate effects of all of the particles at this concentration. However, there were some notable exceptions to these trends. The PRF reaction was actually activated by copper oxide-containing silica, and there were clear differences in the effects of the two types of physisorbed particles. The inhibition of this reaction by physisorbed MCP100 was comparable to that of silica, whereas physisorbed DCB100 inhibited the reaction by approximately 30%.

Another unusual effect associated with the silica and physisorbed nanoparticles, but not with the copper oxide-containing silica, was the activation of the CYP2E1-mediated hydroxylation of *p*-nitrophenol. We found that the activity by this enzyme was inhibited approximately 39% when the saline/tween 80 was tested at 0.09% saline and 0.002% tween (data not shown). Thus, the particles may actually be preventing the inhibition by the detergent rather than stimulating the activity of the enzyme.

With regard to the other reactions, both physisorbed DCB100 and MCP100 inhibited several of the activities by significantly greater levels than those observed in the presence of silica, indicating some specificity in the mechanism of inhibition by the physisorbed particles. However, the inhibition by all of the non-EPFR nanoparticles at 0.2 mg/ml was small in comparison to the levels of inhibition caused by EPFRs (compare Figure 2 with Table 3). Furthermore, this mass concentration is four times higher than the concentration of EPFRs that resulted in greater than 50% inhibition of all of the P450 activities. Thus, it seems unlikely that the effects of the EPFRs can be attributed to the combined effects of copper oxide and physisorbed, halo-aromatic compounds.

Relationship of the free radical concentration of EPFRs and inhibition of AMMC metabolism

EFPRs, because of their stability in the environment, can cause the prolonged propagation of destructive free radical reactions and have been shown to generate superoxide, hydrogen peroxide, and hydroxyl radical when suspended in solution (Khachatryan *et al.*, 2011). To assess whether the inhibition of P450-mediated activities by EPFRs was attributable to the presence of radical species in the particles, we examined the relationship between the level

of P450 inhibition and the free radical concentration of the EPFRs. Figure 3 shows the dose-dependent correlation between the number of radicals from different preparations of EPFRs (MCP230 (panel A) and DCB230 (panel B)) and their abilities to inhibit the CYP2D2-mediated metabolism of AMMC by rat liver microsomes. There was a good linear correlation between the free radical content of the MCP230 and level of inhibition of P450 activity ($r^2 = 0.575$). However, the relationship was not as compelling for DCB230 ($r^2 = 0.34$). Another interesting finding was that the DCB230 had a greater tendency to activate metabolism by CYP2D2 at low concentrations, relative to the effects observed with MCP230. Nevertheless, these data indicate that radicals play an essential role in the nanoparticle-related inhibition of P450 activity.

Effect of catalase on EPFR-related inhibition of P450-mediated activity

To investigate the role of reactive oxygen species in mediating the EPFR-related inhibition of metabolism by CYP2D2, the rates of metabolism of AMMC by rat liver microsomes were determined in the presence and absence of 2000 units/ml catalase (Figure 4). In addition, exposure to copper oxide nanoparticles also has been associated with the generation of reactive oxygen species both *in vivo* (in mussels (Gomes *et al.*, 2011)) and *in vitro* (Fahmy *et al.*, 2009). Thus, the figure also shows the effects of catalase on the inhibition of AMMC dealkylation by copper oxide-containing silica.

In the figure, the EPFR concentrations are listed as the concentration of radicals in exposed media in spins/ml, and the copper oxide-containing silica was tested at 0.4 mg/ml. Consistent with the hypothesis that MCP230 is a more potent inhibitor than DCB230, the former caused greater inhibition of the rate of AMMC metabolism even when it was incubated at a lower radical concentration. The figure shows that 2000 units/ml of catalase attenuated the inhibition of P450-mediated activity by both of the EPFRs. The inhibition by DCB230 and MCP230 were decreased from 60% and 68% in the absence of catalase to 30% and 44% with catalase, respectively. Thus, the data are consistent with the view that EPFR-mediated inhibition of AMMC metabolism is due to the free radical nature of the EPFRs. The generation of reactive oxygen species also seems to relieve at least some of the inhibition by the copper oxide-containing silica as the inhibition by these nanoparticles was decreased from 30% to 20% upon addition of the catalase.

Characterization of the EPFR-related inhibition of AMMC metabolism in rat liver microsomes

Because the metabolism of AMMC by rat liver microsomes appears to be specifically carried out by CYP2D2 and is characterized by Michaelis-Menten kinetics (Makaji *et al.*, 2010; Stresser *et al.*, 2002), we examined this activity in more detail by measuring the microsomal-mediated metabolism as a function of AMMC concentration. By performing a nonlinear regression of the substrate dependence of the rate of AMMC metabolism, we calculated a K_m of CYP2D2 for AMMC of 9.1 μM and a V_{max} of 2.37 nmol/min/mg (which are very close to the kinetic estimates obtained previously (Stresser *et al.*, 2002)). We also measured the rate of AMMC metabolism by rat liver microsomes as a function of AMMC concentration in the presence of various concentrations of EPFRs. The data plotted as Lineweaver-Burk, double reciprocal plots (Figure 5) serve to characterize the mechanism by

which the EPFRs inhibited AMMC metabolism. In the figure, the concentrations of EFPRs are expressed relative to the free radical content (spins/ml) of the particles. Panel A shows that the inhibition of AMMC metabolism by both MCP230 (panel A) and DCB230 (panel B) appeared to be noncompetitive.

Effects of EPFRS on other activities catalyzed by rat liver microsomes

Metabolism mediated by cytochromes P450 requires a physical interaction between the P450s and CPR. Because all of the P450 activities examined were similarly inhibited by the EPFRs, it seemed possible that the mechanism of inhibition may be attributable to a specific effect on the CPR. To test this possibility, we measured the ability of CPR in microsomes from saline-treated rats to reduce cytochrome c (an activity which is specific for CPR when the source of electrons is NADPH). Interestingly, Figure 6 shows that this activity was only inhibited by about 20%, even when incubated at a concentration of 0.2 mg/ml with microsomes which is four-fold higher than that which was found to inhibit more than 50% of all P450 activities examined. Thus, the EPFRs did not markedly inhibit the ability of CPR to transfer electrons to cytochrome c.

The effect of EPFRs on the metabolism of hemin by HO-1 in microsomes from cadmium chloride-induced rats was also determined. Similar to catalysis by P450, the activity of HO-1 is dependent on CPR to transfer electrons to the enzyme. In fact, the HO-1-mediated reaction might be even more dependent on CPR given that its catalytic cycle requires seven electrons, whereas the P450 cycle only needs two electrons to be completed. Figure 7 shows that HO-1 activity was not inhibited by EPFRs at a concentration of 0.2 mg/ml. Interestingly, the activity by HO-1 was actually activated at this concentration of DCB230. It is important to point out, that the same preparations of EPFRs were used for all of the comparative assays reported in the study (Table 2 and Figures 6 and 7). Thus, the EPFRs clearly had a specific effect on P450-mediated metabolism, but did not potently inhibit activities mediated by CPR and HO-1.

Discussion

Other than a few exceptions discussed below, the effects of each type of particle were relatively consistent with respect to the levels by which they inhibited the various P450 activities. More specifically, EPFRs inhibited the rate of metabolism by each of the P450s by more than 50% at a concentration of 0.05 mg/ml – a concentration where none of the control particles showed inhibition (Figure 2 & Table 3). In general, inhibition by the control particles were only observed at significantly higher particle concentrations. Such data strongly support the idea that some unique characteristic of the EPFRs is responsible for the more potent inhibition of P450 activities, and not simply the presence of nanoparticles in the incubation.

Previously, similar levels of inhibition of metabolism by different human P450s expressed in Baculosomes© were also associated with coarse (≈ 10 nm in diameter) metallic nanoparticles (Sereemaspun *et al.*, 2008), where it was proposed that the particles inhibited the P450-mediated metabolism by forming mixed micelles that altered the structure of the membrane lipid bilayer and in turn, disrupted the ability of the enzymes to interact with CPR

and function (Sereemaspun *et al.*, 2008). Another study speculated that this particle-related membrane disruption also could impair the interaction of hydrophobic substrates and P450s (Frohlich *et al.*, 2010).

Although membrane disruption may be a mechanism by which the non-EPFR particles inhibit P450-mediated metabolism, other mechanisms are likely involved in the more potent inhibition found in the presence of EPFRs. There are several reasons for this conclusion. First, if membrane disruption was the mechanism common to all the particles, we would expect similar degrees of inhibition both by EPFR and non-EPFRs. Second, a particle-related alteration of membrane structure also would be expected to inhibit activity by HO-1; however, the particles had no effect on this activity at concentrations of 0.2 mg/ml. Third, inhibition of AMMC dealkylation by EPFRs was shown to be attenuated by the presence of catalase, suggesting a role for reactive oxygen species in the mechanism of inhibition (Figure 4). Thus, membrane disruption may partly explain the inhibition by non-EPFRs, but probably not the more potent inhibition by EPFRs.

Currently, the prevailing evidence suggests that most of the health effects of EFPRs are attributed to their ability to generate reactive oxygen species (Dellinger *et al.*, 2000; Dellinger *et al.*, 2001). It has been demonstrated that EPFRs in solution can react with molecular oxygen to form superoxide and hydroxyl radicals in an acyclic process. Superoxide can dismutate to form hydrogen peroxide. In a reaction analogous to the Fenton reaction, radical cuprous ion can react with hydrogen peroxide to form hydroxide ion and the highly destructive hydroxyl radical (Khachatryan *et al.*, 2011). Catalase significantly attenuated the level of inhibition by both types of EPFRs. Thus, it seems likely that the more potent inhibition of P450-mediated metabolism by EPFRs is related to the generation of reactive oxygen species.

Catalase was only partially effective in eliminating the EPFR-related inhibiton of P450. It is possible that higher concentrations of catalase may have resulted in more complete recovery of the P450 activity. Alternatively, the data may be an indication that another reactive oxygen species such as superoxide is involved in the mechanism of inhibition. It also seems possible that the radicals contained by the EPFRs may interact directly with the P450s and contribute to the total inhibition of activity. As shown previously (Fahmy *et al.*, 2009; Gomes *et al.*, 2011), reactive oxygen species can also be formed in the presence of the copper oxide-containing silica when the nanoparticle interacts with cellular enzymes. This would explain both the more potent inhibition by copper oxide-containing silica (relative to free silica and physisorbed nanoparticles) and the ability of catalase to attenuate the inhibition by copper oxide-containing silica. Unlike EPFRs, the copper oxide-containing silica would require some type of enzymatic reduction of the metal group by the microsomes before reactive oxygen species could be formed. This would explain why the inhibition of P450 by these particles was less potent than that by the EPFRs. Further evidence for an increase in reactive oxygen species in the presence of the copper oxide-containing silica was likely demonstrated in the effects of 0.2 mg/ml of the nanoparticle on CYP2B-mediated metabolism of PRF (Table 3). This reaction is dependent on a redox cycle involving CPR, PRF, and either molecular oxygen or superoxide (Dutton *et al.*, 1989), and it was postulated that low levels of superoxide could stimulate the rate of product formation. Thus, it seems

possible that the stimulation of PRF metabolism in the presence of low concentrations of copper oxide-containing silica was caused by a particle-related increase in superoxide.

Our data indicate that the effects of the nanoparticles are complex and cannot be attributable to one general mechanism of inhibition. Copper oxide-containing silica has effects that are distinct from those associated with the EPFRs. Furthermore, the two types of physisorbed nanoparticles had effects that were also distinct from those of silica. In fact, the two types of EPFRs also were distinguished by their effects with MCP230 being more potent than DCB230 (Table 2 and Figure 3). When metabolism by CYP2D2 was examined as a function of AMMC concentration, inhibition by both MCP230 and DCB230 generally appeared to be non-competitive.

Because reactive oxygen species are involved in the mechanism of inhibition of P450 by EPFRs, it may be assumed that the reactive oxygen species are damaging the P450 and causing irreversible inhibition of the enzyme activities. However, all of the enzymatic assays in this study were conducted in real time and were linear for the entire length of the assay (> 5 min). Thus, it appears that the inhibition by EPFRs is reversible unless the EPFRs quickly inactivated (before reactions were initiated with NADPH) only a fraction of P450 that was proportional to the EPFR concentration. This latter possibility seems unlikely, so we believe the inhibition by EPFRs is reversible.

This study adds to the findings of previous research with respect to the effects of particles on P450-mediated activities in vitro. Previously, it was shown that gold and silver nanoparticles (≈ 10 nm in diameter) generally and consistently inhibited metabolism by human CYP1A2, CYP2C9, CYP2C19, and CYP3A4 (Sereemaspun *et al.*, 2008) (discussed above). In addition, gold nanoparticles were found to inhibit more than silver nanoparticles. Interestingly, another study using carboxyl polystyrene particles found their inhibitory effects to be both P450-selective and size-dependent (Frohlich *et al.*, 2010). Inhibition was only observed with carboxyl polystyrene particles that were 60 nm in diameter or smaller. Activities by human CYP2C9, CYP2D6, and CYP3A4 were inhibited between 20 and 45% by this size range of particles at concentrations less than 100 μg/ml. At 200 μg/ml, more pronounced inhibition of the activities (60–100%) was observed with the 20 nm (but not with the 60 nm) carboxyl polystyrene particles. In contrast to our results with EPFRs, CYP1A2-mediated metabolism was refractory to the effects of the carboxyl-polystyrene particles at all concentrations tested (≤ 200 μg/ml). The lack of inhibition from the particle used in the current study may be a consequence of their larger size (200 nm), where we found little to no inhibitory effect on P450 activities.

Our study has enhanced the understanding of particle effects on P450 enzymes by examining a variety of particle types. These findings indicate that the effects of nanoparticles can be diverse and dependent on the particle type. Unlike previous reports, we have assessed the role of reactive oxygen species in the inhibition of P450-mediated activity by EFPRs. P450 inhibition by EPFRs seems to be predominantly a function of the concentration and reactivity of the radicals bound to the particles and appears to be related to the production of reactive oxygen species. Finally, by using rat liver microsomes as opposed to recombinant P450 expressed in Baculosomes, we have been able to assess the effects of

particles in a natural system that contains the proportions of P450 and CPR that are present in vivo. Thus, we have demonstrated the effects of particles on P450 activities while allowing for the potential influences of protein protein interactions and the limiting supply of CPR that exist in the natural membranes (Reed *et al.*, 2010; Reed *et al.*, 2012a; Reed *et al.*, 2012b). By using this approach, we have also been able to assess the effects of particles on another enzyme system that utilizes CPR, the HO-1. Unlike P450, activity by HO-1 was not affected by particles even at a concentration that was 4-fold greater than that needed to inhibit more than 50% of all P450-related activities.

The inhalation of fine and ultrafine particles leads to their systemic distribution and accumulation in various tissues (Kreyling *et al.*, 2009; Nemmar *et al.*, 2002; Oberdorster *et al.*, 2005). Particles as large as 240 nm have been shown to be translocated from the interstitial lung epithelium into systemic circulation after inhalation (Kato *et al.*, 2003). Diesel exhaust particles, like EPFRs, are generated through a process of combustion in which particulate matter is heated with reactive aromatic hydrocarbons. These particles have been shown to both induce and repress expression of different types of P450s in lungs (Ma *et al.*, 2002){Rengasamy, 2003 1763/id; Hatanaka, 2001 1761/id}, livers (Hatanaka *et al.*, 2001), and kidneys (Hatanaka *et al.*, 2001) in animals exposed to these particles by inhalation or instillation. Because EPFRs were found to inhibit P450-mediated metabolism, our study raises the possibility of additional the health risks associated with exposure to nanoparticles as the individuals exposed to particles might be compromised in their ability to metabolize drugs and other xenobiotics. Interestingly, the exposure to EPFRs could have competing effects in cells, particularly in cases when EPFRs induce expression of P450 forms. If the EPFRs are present at sufficient concentrations when the enzymes are induced, enzyme activities would be inhibited, and the effects of enzyme induction would not be manifest. Thus, the end result of exposure to EPFRs, in terms of xenobiotic metabolism, will depend on the timing of elimination of the EPFRs from the cells and the induction of P450 forms. Thus, enzyme induction alone may not have predictable consequences following EPFR exposure, and future studies with nanoparticles should carefully investigate the interplay of P450 expression and activities when assessing the effects of the particles.

Acknowledgments

Funding

This work was supported by US Public Health Service Research Grants from the National Institute of Environmental Health Sciences [ES013648 to WLB, JRR and ES004344 to WLB].

Abbreviations

EPFRs	environmentally persistent free radicals
MCP230	EPFR generated by heating vapors of 2-monochlorophenol with copper oxide-containing silica to 230°C under vacuum
MCP100	non-radical silica nanoparticles containing physisorbed 2-monochlorophenol prepared by heating vapors of 2-monochlorophenol with silica to 100°C under vacuum

DCB230	EPFR generated by heating vapors of 1,2-dichlorobenzene with copper oxide-containing silica to 230°C under vacuum
DCB100	non-radical silica nanoparticles containing physisorbed 1,2-dichlorobenzene prepared by heating vapors of 1,2-dichlorobenzene with silica to 100°C under vacuum
CYP or P450	cytochrome P450
CPR	cytochrome P450 reductase
HO-1	heme oxygenase 1
BNF	β-naphthoflavone
ANF	α-naphthoflavone
PNP	*p*-nitrophenol
MRF	7-methoxyresorufin
BQ	7-benzyloxyquinoline
PRF	7-pentoxyresorufin
CEC	3-cyano-7-ethoxycoumarin
AMMC	3-[2-(N,N-diethyl-N-methylammonium)ethyl]-7-methoxy-4-methylcoumarin
CHC	3-cyano-7-hydroxycoumarin
AHMC	3-[2-(diethylamino)ethyl]-7-hydroxy-4-methylcoumarin hydrochloride

Reference List

Allis JW, Robinson BL. A kinetic assay for p-nitrophenol hydroxylase in rat liver microsomes. Analytical Biochemistry. 1994; 219:49–52. [PubMed: 8059955]

Balakrishna S, Lomnicki S, McAvey KM, Cole RB, Dellinger B, Cormier SA. Environmentally persistent free radicals amplify ultrafine particle mediated cellular oxidative stress and cytotoxicity. Part Fibre Toxicol. 2009; 6:11. [PubMed: 19374750]

Balakrishna S, Saravia J, Thevenot P, Ahlert T, Lominiki S, Dellinger B, Cormier SA. Environmentally persistent free radicals induce airway hyperresponsiveness in neonatal rat lungs. Part Fibre Toxicol. 2011; 8:11. [PubMed: 21388553]

Barham HM, Lennard MS, Tucker GT. An evaluation of cytochrome P450 isoform activities in the female dark agouti (DA) rat: relevance to its use as a model of the CYP2D6 poor metaboliser phenotype. Biochemical Pharmacology. 1994; 47:1295–1307. [PubMed: 8185638]

Brook RD, Rajagopalan S, Pope CA III, Brook JR, Bhatnagar A, Diez-Roux AV, Holguin F, Hong Y, Luepker RV, Mittleman MA, Peters A, Siscovick D, Smith SC Jr, Whitsel L, Kaufman JD. Particulate matter air pollution and cardiovascular disease: An update to the scientific statement from the American Heart Association. Circulation. 2010; 121:2331–2378. [PubMed: 20458016]

Burke MD, Prough RA, Mayer RT. Characteristics of a microsomal cytochrome P-448-mediated reaction. Ethoxyresorufin O-de-ethylation. Drug Metab Dispos. 1977; 5:1–8. [PubMed: 13970]

Burke MD, Thompson S, Elcombe JR, Halpert J, Haaparanta T, Mayer RT. Ethoxy-Pentoxy-and Benzyloxyphenoxazones and Homologues: A Series of Substrates to Distinguish Between Different Induced Cytochromes P-450. Biochemical Pharmacology. 1985; 34:3337–3345. [PubMed: 3929792]

Burke MD, Thompson S, Weaver RJ, Wolf CR, Mayer RT. Cytochrome P450 specificities of alkoxyresorufin O-dealkylation in human and rat liver. Biochemical Pharmacology. 1994; 48:923–936. [PubMed: 8093105]

Cass GR, Hughes LA, Bhave P, Kleeman MJ, Allen JO, Salmon LG. The chemical composition of atmospheric ultrafine particles. Philos Transact A Math Phys Eng Sci. 2000; 358:2581–2592.

Cawley GF, Zhang S, Kelley RW, Backes WL. Evidence supporting the interaction of CYP2B4 and CYP1A2 in microsomal preparations. Drug Metab Dispos. 2001; 29:1529–1534. [PubMed: 11717170]

Cormier SA, Lomnicki S, Backes W, Dellinger B. Origin and health impacts of emissions of toxic by-products and fine particles from combustion and thermal treatment of hazardous wastes and materials. Environmental Health Perspectives. 2006; 114:810–817. [PubMed: 16759977]

Dellinger, B.; Pryor, WA.; Cueto, R.; Squadrito, GL.; Deutsch, WA. The role of combustion-generated radicals in the toxicity of PM2.5. Proceedings of the International Sumposium on Combustion; 2000.

Dellinger B, Pryor WA, Cueto R, Squadrito GL, Hegde V, Deutsch WA. Role of free radicals in the toxicity of airborne fine particulate matter. Chemical Research in Toxicology. 2001; 14:1371–1377. [PubMed: 11599928]

Dockery DW. Epidemiologic evidence of cardiovascular effects of particulate air pollution. Environmental Health Perspectives. 2001; 109:483–486. [PubMed: 11544151]

Dutton DR, Parkinson A. Reduction of 7-alkoxyresorufins by NADPH-cytochrome P450 reductase and its differential effects on their O-dealkylation by rat liver microsomal cytochrome P450. Archives of Biochemistry and Biophysics. 1989; 268:617–629. [PubMed: 2536534]

Fahmy B, Cormier SA. Copper oxide nanoparticles induce oxidative stress and cytotoxicity in airway epithelial cells. Toxicol In Vitro. 2009; 23:1365–1371. [PubMed: 19699289]

Frohlich E, Kueznik T, Samberger C, Roblegg E, Wrighton C, Pieber TR. Size-dependent effects of nanoparticles on the activity of cytochrome P450 isoenzymes. Toxicology and Applied Pharmacology. 2010; 242:326–332. [PubMed: 19909766]

Gauderman WJ, Avol E, Gilliland F, Vora H, Thomas D, Berhane K, McConnell R, Kuenzli N, Lurmann F, Rappaport E, Margolis H, Bates D, Peters J. The effect of air pollution on lung development from 10 to 18 years of age. N Engl J Med. 2004; 351:1057–1067. [PubMed: 15356303]

Gomes T, Pinheiro JP, Cancio I, Pereira CG, Cardoso C, Bebianno MJ. Effects of copper nanoparticles exposure in the mussel Mytilus galloprovincialis. Environ Sci Technol. 2011; 45:9356–9362. [PubMed: 21950553]

Guengerich FP. Common and uncommon cytochrome P450 reactions related to metabolism and chemical toxicity. Chemical Reserarch in Toxicology. 2001; 14:611–650.

Hatanaka N, Yamazaki H, Kizu R, Hayakawa K, Aoki Y, Iwanari M, Nakajima M, Yokoi T. Induction of cytochrome P450 1B1 in lung, liver and kidney of rats exposed to diesel exhaust. Carcinogenesis. 2001; 22:2033–2038. [PubMed: 11751436]

Howard LA, Micu AL, Sellers EM, Tyndale RF. Low doses of nicotine and ethanol induce CYP2E1 and chlorzoxazone metabolism in rat liver. Journal of Pharmacology and Experimental Therapeutics. 2001; 299:542–550. [PubMed: 11602665]

Hwang JS, Chan CC. Effects of air pollution on daily clinic visits for lower respiratory tract illness. American Journal of Epidemiology. 2002; 155:1–10. [PubMed: 11772777]

Kato T, Yashiro T, Murata Y, Herbert DC, Oshikawa K, Bando M, Ohno S, Sugiyama Y. Evidence that exogenous substances can be phagocytized by alveolar epithelial cells and transported into blood capillaries. Cell Tissue Res. 2003; 311:47–51. [PubMed: 12483283]

Kennedy IM. The health effects of combustion-generated aerosols. Proc Combust Inst. 2007; 31:2757–2770.

Khachatryan L, Vejerano E, Lomnicki S, Dellinger B. Environmentally persistent free radicals (EPFRs). 1 Generation of reactive oxygen species in aqueous solutions. Environ Sci Technol. 2011; 45:8559–8566. [PubMed: 21823585]

Koop DR, Crump BL, Nordblom GD, Coon MJ. Immunochemical evidence for induction of the alcohol-oxidizing cytochrome P-450 of rabbit liver microsomes by diverse agents: ethanol,

imidazole, trichloroethylene, acetone, pyrazole, and isoniazid. Proc Natl Acad Sci USA. 1985; 82:4065–4069. [PubMed: 3858864]

Koop DR, Laethem CL, Tierney DJ. The utility of p-nitrophenol hydroxylation in P450IIE1 analysis. Drug Metab Rev. 1989; 20:541–551. [PubMed: 2680397]

Koop DR, Tierney DJ. Multiple mechanisms in the regulation of ethanol-inducible cytochrome P450IIE1. Bioessays. 1990; 12:429–435. [PubMed: 2256907]

Kreyling WG, Semmler-Behnke M, Seitz J, Scymczak W, Wenk A, Mayer P, Takenaka S, Oberdorster G. Size dependence of the translocation of inhaled iridium and carbon nanoparticle aggregates from the lung of rats to the blood and secondary target organs. Inhal Toxicol. 2009; 21(Suppl 1): 55–60. [PubMed: 19558234]

Liu J, Ericksen SS, Sivaneri M, Besspiata D, Fisher CW, Szklarz GD. The effect of reciprocal active site mutations in human cytochromes P450 1A1 and 1A2 on alkoxyresorufin metabolism. Archives of Biochemistry and Biophysics. 2004; 424:33–43. [PubMed: 15019834]

Loida PJ, Sligar SG. Molecular recognition in cytochrome P-450: mechanism for the control of uncoupling reactions. Biochemistry. 1993; 32:11530–11538. [PubMed: 8218220]

Lomnicki S, Dellinger B. A Detailed Mechanism of The Surface-Mediated Formation of PCDD/F from the Oxidation of 2-Chlorophenol on CuO/Silica Surface. Journal of Physical Chemistry. 2003; 107:4387–4395.

Lomnicki S, Truong H, Vejerano E, Dellinger B. Copper oxide-based model of persistent free radical formation on combustion-derived particulate matter. Environ Sci Technol. 2008; 42:4982–4988. [PubMed: 18678037]

Lord K, Moll D, Lindsey JK, Mahne S, Raman G, Dugas T, Cormier S, Troxlair D, Lomnicki S, Dellinger B, Varner K. Environmentally persistent free radicals decrease cardiac function before and after ischemia/reperfusion injury in vivo. J Recept Signal Transduct Res. 2011; 31:157–167. [PubMed: 21385100]

Ma JYC, Ma JKH. The dual effect of the particulate and organic components of diesel exhaust particles on the alteration of pulmonary immune/inflammatory responses and metabolic enzymes. J Environm Sci Health. 2002; C20:117–147.

Maestrelli P, Canova C, Scapellato ML, Visentin A, Tessari R, Bartolucci GB, Simonato L, Lotti M. Personal exposure to particulate matter is associated with worse health perception in adult asthma. J Investig Allergol Clin Immunol. 2011; 21:120–128.

Mahne S, Chuang GC, Pankey E, Kiruri L, Kadowitz PJ, Dellinger B, Varner KJ. Environmentally persistent free radicals decrease cardiac function and increase pulmonary artery pressure. Am J Physiol Heart Circ Physiol. 2012; 303:H1135–H1142. [PubMed: 22942180]

Maines MD. Carbon monoxide and nitric oxide homology: Differential modulation of heme oxygenases in brain and detection of protein and activity. Methods Enzymol. 1996; 268:473–488. [PubMed: 8782613]

Makaji E, Trambitas CS, Shen P, Holloway AC, Crankshaw DJ. Effects of cytochrome P450 inhibitors on the biotransformation of fluorogenic substrates by adult male rat liver microsomes and cDNA-expressed rat cytochrome P450 isoforms. Toxicol Sci. 2010; 113:293–304. [PubMed: 19858067]

Nelson DR. Comparison of P450s from human and fugu: 420 million years of vertebrate P450 evolution. Archives of Biochemistry and Biophysics. 2003; 409:18–24. [PubMed: 12464240]

Nemmar A, Hoet PH, Vanquickenborne B, Dinsdale D, Thomeer M, Hoylaerts MF, Vanbilloen H, Mortelmans L, Nemery B. Passage of inhaled particles into the blood circulation in humans. Circulation. 2002; 105:411–414. [PubMed: 11815420]

Nemmar A, Vanbilloen H, Hoylaerts MF, Hoet PH, Verbruggen A, Nemery B. Passage of intratracheally instilled ultrafine particles from the lung into the systemic circulation in hamster. Am J Respir Crit Care Med. 2001; 164:1665–1668. [PubMed: 11719307]

Nerurkar PV, Park SS, Thomas PE, Nims RW, Lubet RA. Methoxyresorufin and benzyloxyresorufin: substrates preferentially metabolized by cytochromes P4501A2 and 2B, respectively, in the rat and mouse. Biochemical Pharmacology. 1993; 46:933–943. [PubMed: 8373445]

Oberdorster G, Oberdorster E, Oberdorster J. Nanotoxicology: an emerging discipline evolving from studies of ultrafine particles. Environmental Health Perspectives. 2005; 113:823–839. [PubMed: 16002369]

Phillips AH, Langdon RG. Hepatic triphosphopyridine nucleotide-cytochrome c reductase: isolation, characterization, and kinetic studies. Journal of Biological Chemistry. 1962; 237:2652–2660. [PubMed: 14486217]

Pope CA III, Burnett RT, Thun MJ, Calle EE, Krewski D, Ito K, Thurston GD. Lung cancer, cardiopulmonary mortality, and long-term exposure to fine particulate air pollution. JAMA. 2002; 287:1132–1141. [PubMed: 11879110]

Reed JR, Backes WL. Formation of P450. P450 complexes and their effect on P450 function. Pharmacology and Therapeutics. 2012a; 133:299–310. [PubMed: 22155419]

Reed JR, Cawley GF, Backes WL. Inhibition of cytochrome P450 1A2-mediated metabolism and production of reactive oxygen species by heme oxygenase-1 in rat liver microsomes. Drug Metab Lett. 2011; 5:6–16. [PubMed: 20942796]

Reed JR, Connick JP, Cheng D, Cawley GF, Backes WL. Effect of Homomeric P450 P450 Complexes on P450 Function. Biochemical Journal. 2012b; 446:489–497. [PubMed: 22738171]

Reed JR, Eyer M, Backes WL. Functional interactions between cytochromes P450 1A2 and 2B4 require both enzymes to reside in the same phospholipid vesicle: evidence for physical complex formation. Journal of Biological Chemistry. 2010; 285:8942–8952. [PubMed: 20071338]

Reidy GF, Mehta I, Murray M. Inhibition of oxidative drug metabolism by orphenadrine: in vitro and in vivo evidence for isozyme-specific complexation of cytochrome P-450 and inhibition kinetics. Molecular Pharmacology. 1989; 35:736–743. [PubMed: 2725477]

Rengasamy A, Barger MW, Kane E, Ma JK, Castranova V, Ma JY. Diesel exhaust particle-induced alterations of pulmonary phase I and phase II enzymes of rats. J Toxicol Environ Health A. 2003; 66:153–167. [PubMed: 12653020]

Renwick AB, Lavignette G, Worboy PD, Williams B, Surry D, Lewis DF, Price RJ, Lake BG, Evans DC. Evaluation of 7-benzyloxy-4-trifluoromethylcoumarin, some other 7-hydroxy-4-trifluoromethylcoumarin derivatives and 7-benzyloxyquinoline as fluorescent substrates for rat hepatic cytochrome P450 enzymes. Xenobiotica. 2001; 31:861–878. [PubMed: 11780761]

Sereemaspun A, Hongpiticharoen P, Rojanathanes R, Maneewattanapinyo P, Ekgasit S, Warisnoicharoen W. Inhibition of human cytochrome P450 enzymes by metallic nanoparticles: a preliminary to nanogenomics. Int J Pharmacol. 2008; 4:492–495.

Stresser DM, Turner SD, Blanchard AP, Miller VP, Crespi CL. Cytochrome P450 fluorometric substrates: identification of isoform-selective probes for rat CYP2D2 and human CYP3A4. Drug Metab Dispos. 2002; 30:845–852. [PubMed: 12065444]

Turan VK, Mishin VM, Thomas PE. Clotrimazole is a selective and potent inhibitor of rat cytochrome P450 3A subfamily-related testosterone metabolism. Drug Metab Dispos. 2001; 29:837–842. [PubMed: 11353752]

White RE, Coon MJ. Oxygen activation by cytochrome P-450. Annu Rev Biochem. 1980; 49:315–356. [PubMed: 6996566]

Wiebel FJ, Leutz JC, Diamond L, Gelboin HV. Aryl hydrocarbon (benzo(a)pyrene) hydroxylase in microsomes from rat tissues: differential inhibition and stimulation by benzoflavones and organic solvents. Archives of Biochemistry and Biophysics. 1971; 144:78–86. [PubMed: 5117540]

Highlights

- Combustion of organic pollutants generates long-lived particulate radicals (EPFRs).
- EPFRs inhibit metabolism by all cytochromes P450 tested in rat liver microsomes.
- EPFR-mediated inhibition is related to spin content and is sensitive to catalase.
- EPFR inhibition of CYP2D2 is noncompetitive with respect to substrate.
- Exposure to EPFRs may impair the ability to eliminate xenobiotics.

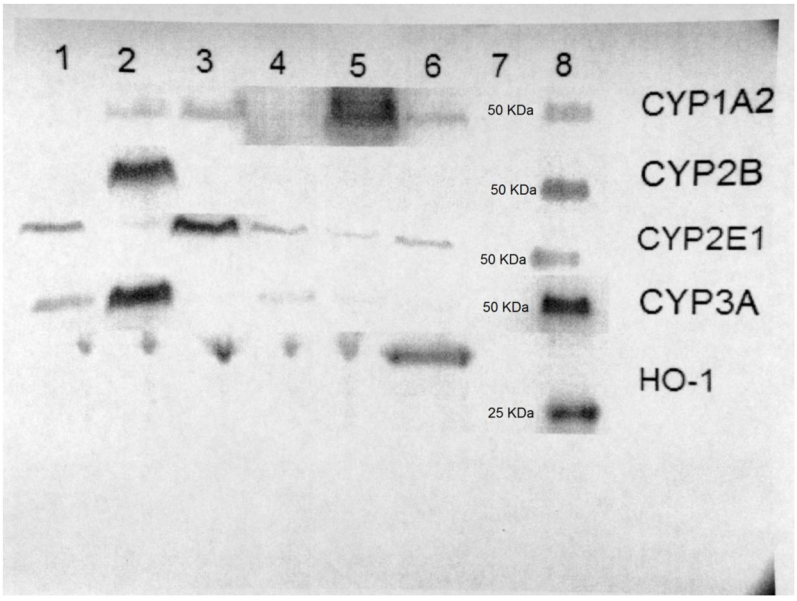

Figure 1.

Western blots showing levels of expression of HO-1 and different forms of P450 in liver microsomes from rats treated with various inducing agents. Western blots were performed as indicated in Materials and Methods. The image shows cross-sections of five western blots for each of the inducible enzymes that were tested in this study and demonstrates that chemical treatments successfully induced the desired enzymes. The primary antibodies specific to the individual enzymes (described in Materials and Methods) were used as indicated in the different rows of gel images. The samples shown in lanes one through six were derived from rats treated with saline, phenobarbital, pyrazole, corn oil, β-naphthoflavone, and cadmium chloride, respectively. Lane 7 was blank. A molecular weight ladder was run in lane 8, and the band in the lanes for P450 blots is the 50 kDa marker, whereas that in the HO-1 blot is the 25 kDa marker. The molecular weight of the ladder for each of the five western blots is indicated in lane 7.

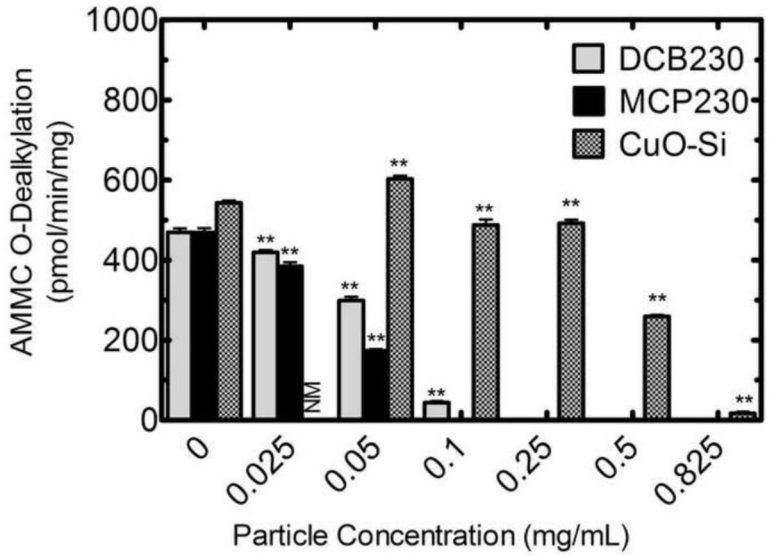

Figure 2.

Rates of AMMC *O*-dealkylation as a function of particle concentration. Rates of AMMC *O*-dealkylation by liver microsomes from saline-treated rats with or without the indicated concentrations of MCP230, DCB230, and copper oxide-containing silica particles (CuO-Si) were measured as indicated in Materials and Methods. The rates indicate the average ± the standard error of three determinations. ** indicates that the rates were significantly different from the corresponding groups in the absence of particles ($P < 0.01$). All assays contained 0.68% saline and 0.015% Tween-80. NM – not measured.

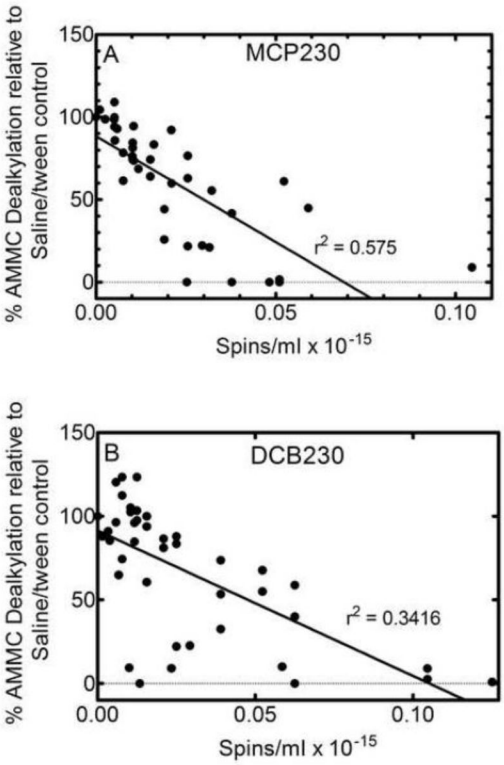

Figure 3.

Rates of AMMC *O*-dealkylation as a function of the concentration of radicals (spins/ml $x10^{-15}$) associated with either MCP230 (panel A) or DCB230 (panel B). Rates of AMMC *O*-dealkylation by liver microsomes from saline-treated rats were determined in the presence or absence of EPFRs as described in Materials and Methods. The spin contents of the EPFRs were determined by ESR as described in Materials and Methods. The data represent the concentration-dependent effects of radicals from eight batches of MCP230 and eleven batches of DCB230 prepared over an eight month interval. Linear regressions of the data were performed using Prism 5.02 (GraphPad, La Jolla, CA).

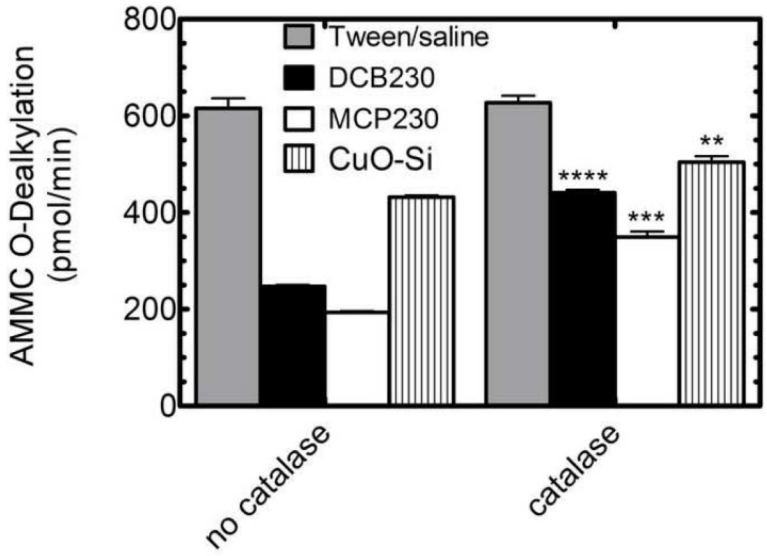

Figure 4.

Effects of EPFRs, copper oxide-containing silica (CuO-Si), and catalase on the rates of AMMC *O*-dealkylation by rat liver microsomes. Rates of AMMC *O*-dealkylation by liver microsomes from saline-treated rats were determined in the presence or absence of EPFRs. The amounts of MCP230 and DCB230 used were based on the number of spins as determined by EPR (2.5×10^{17} and 6.2×10^{17} spins/ml, respectively). CuO-Si was used at a concentration that could inhibit AMMC metabolism (0.4 mg/ml). Reactions also were performed in the presence and absence of 2000 units/ml catalase as indicated. The rates represent the averages ± the standard error of three separate determinations. **, ***, **** indicate that the rates are significantly different from the corresponding control incubations without catalase ($p < 0.01$, $p < 0.001$, and $p < 0.0001$, respectively).

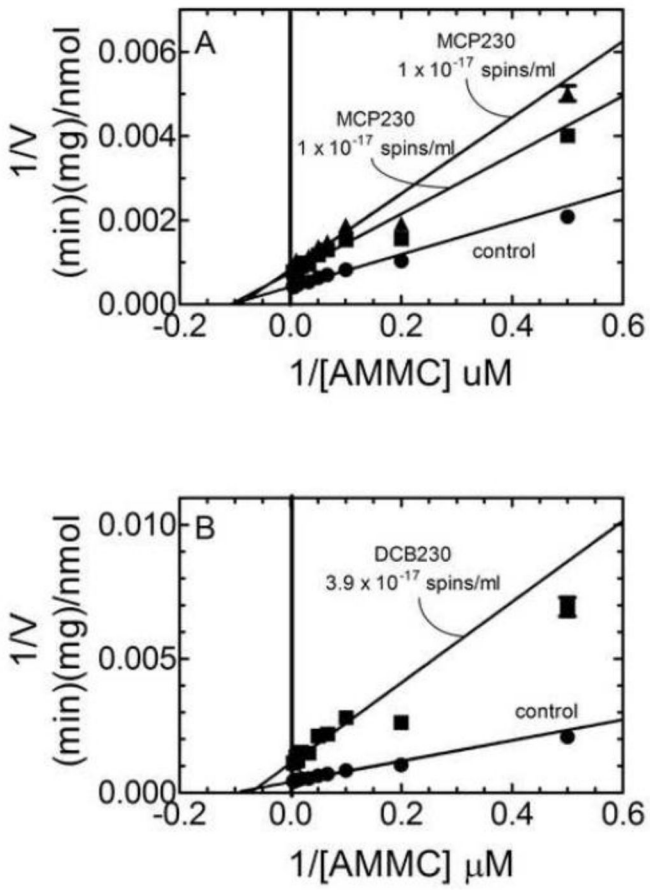

Figure 5.

Double reciprocal plots of the rates of AMMC *O*-dealkylation as a function the concentration of AMMC in the presence and absence of MCP230 (panel A) and DCB230 (panel B) at various spin concentrations. The rates of AMMC *O*-dealkylation by liver microsomes from saline-treated rats were determined as a function of AMMC concentration in the presence or absence of EPFRs (incubated at the indicated spin concentration) as described in Materials and Methods. Each data point represents reciprocals of the average rate of metabolism ± the standard error of three determinations. The lines were generated by non-linear regressions of the untransformed data using the Michaelis-Menten equation and plotted as double reciprocals.

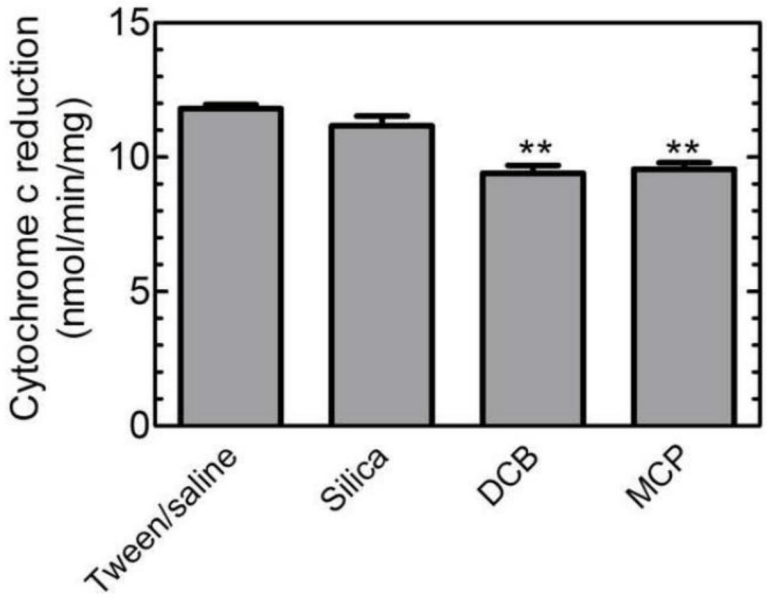

Figure 6.

Rates of cytochrome c reduction by liver microsomes from saline-treated rats in the presence and absence of different types of particles. The rates of cytochrome c reduction by microsomes from saline-treated rats were determined in the presence and absence of 0.2 mg/ml of MCP230 (12.7×10^{17} spins/ml), DCB230 (2.7×10^{17} spins/ml) and silica. All incubations contained the same concentrations of saline and Tween 80. The rates represent the averages ± the standard errors of three separate determinations. ** indicates results that are significantly different from control reactions not containing particles ($P < 0.01$).

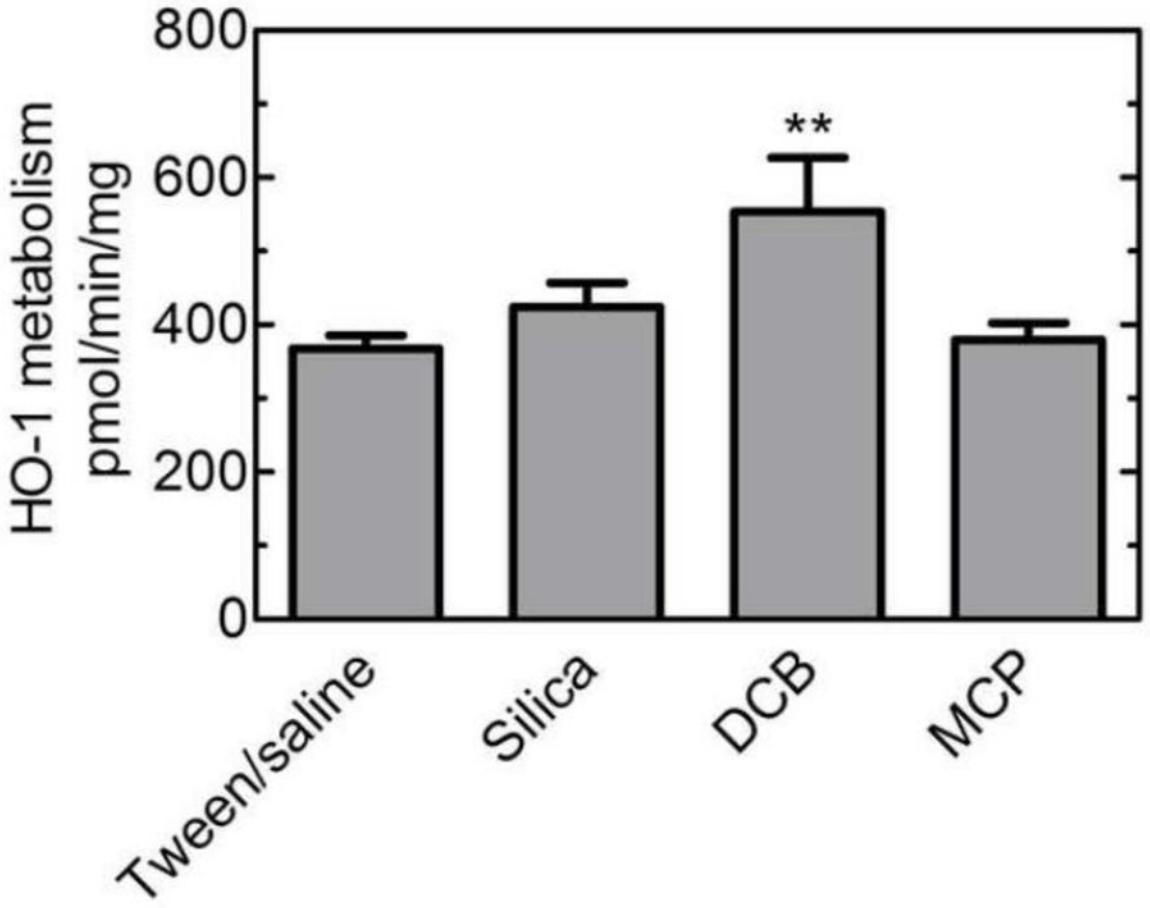

Figure 7.

Rates of heme degradation by liver microsomes from cadmium chloride-treated rats in the presence and absence of different types of particles. The rates of heme degradation by microsomes from cadmium chloride-treated rats were determined in the presence and absence of 0.2 mg/ml of MCP230 (12.7 x 10^{17} spins/ml), DCB230 (2.7 x 10^{17} spins/ml) and silica. All incubations contained the same concentrations of saline and Tween 80. The rates represent the averages ± the standard errors of three determinations. ** indicates results that are significantly different from control reactions not containing particles ($P < 0.01$).

Table 1

Microsomal-mediated metabolism of probe substrates and effects of specific chemical inhibitors of different forms of P450[1]

P450 form	Substrate (μM)	Activity − Inhibitor (nmol/min/mg)	Inhibitor (μM)	Activity + Inhibitor (nmol/min/mg)
CYP1A1	CEC (40)[2]	18.30 ± 0.24[3]	ANF (10)	0.87 ± 0.02
CYP1A2	MRF (5)	0.18 ± 0.004	ANF (10)	0.003 ± 0.001
CYP2B	PRF (5)	0.86 ± 0.01	Orphenadrine (40)	0.08 ± 0.001
CYP2E1	PNP (100)	2.20 ± 0.13	Chloroxazone (500)	0.61 ± 0.14
CYP2D2	AMMC (20)	0.70 ± 0.002	Quinine (1)	N.D.[4]
CYP3A	BQ (40)	6.63 ± 0.07	Clotrimazole (0.1)	0.98 ± 0.02

[1] The conditions used to measure the rates of metabolism of probe substrates by different types of rat liver microsomes are specified in Materials and Methods.

[2] The numbers in parentheses indicate the concentrations at which the substrates and inhibitors were incubated in the enzymatic assays.

[3] Rates represent the average ± the standard error of three separate determinations.

[4] N.D. indicates not detected.

Toxicol Appl Pharmacol. Author manuscript; available in PMC 2015 June 01.

Table 2

Effects of EPFRs and silica on P450-specific metabolism of probe substrates in rat liver microsomes[1].

P450 form	Substrate (μM)[2]	Control Rate[3]	DCB230[4] (% of control)	MCP230 (% of control)	Silica
CYP1A1	CEC (40)	9.39 ± 0.08	1.94 ± 0.01** (20%)	0.73 ± 0.02** (8%)	9.35 ± 0.24
CYP1A2	MRF (5)	0.085 ± 0.002	0.009 ± 0.001** (11%)	0.007 ± 0.0002** (8%)	0.087 ± 0.003
CYP2B	PRF (5)	1.91 ± 0.10	0.29 ± 0.01** (15%)	0.11 ± 0.002** (6%)	2.10 ± 0.01
CYP2E1	PNP (100)	2.38 ± 0.19	0.11 ± 0.06** (5%)	0.35 ± 0.10** (15%)	2.05 ± 0.27
CYP2D2	AMMC (20)	0.411 ± 0.009	0.13 ± 0.01** (32%)	0.08 ± 0.01** (20%)	0.40 ± 0.012
CYP3A	BQ (40)	4.60 ± 0.04	2.21 ± 0.03** (48%)	1.25 ± 0.17** (27%)	4.46 ± 0.07

[1]The conditions used to measure the effects of particles on the rates of metabolism of probe substrates by different types of rat liver microsomes are specified in Materials and Methods. The control reactions did not contain any nanoparticles but did contain an equal volume of the saline-Tween 80 solution that was used to suspend the particles. The final concentrations of saline and Tween 80 in all reactions were 0.023% and 0.0005%, respectively.

[2]The numbers in parentheses in column 2 indicate the concentrations at which the substrates were incubated in the enzymatic assays.

[3]Rates represent the average ± the standard error of three separate determinations and are expressed as nmol/min/mg of microsomal protein. ** indicates the results are significantly different from the control ($P < 0.01$).

[4]EPFRs (DCB230 and MCP230) and silica particles were incubated at 0.05 mg/ml in the enzymatic reactions with probe substrates.

Table 3

Relative rates of metabolism of probe substrates in the presence of 0.2 mg/ml of fumed silica, silica with 5% copper oxide or physisorbed MCP100[1]

P450 form	Substrate (μM)	CuO-Si[2] % of control	Silica % of control	DCB100 Physisorbed % of control	MCP100 Physisorbed % of control
CYP1A1	CEC (40)	90 ± 2*	93 ± 0.4	98 ± 3	97 ± 3
CYP1A2	MRF (5)	92 ± 3	95 ± 1	91 ± 2*	89 ± 1**,+
CYP2B	PRF (5)	126 ± 1***	86 ± 0.2**	69 ± 0.4***,+++	83 ± 1**
CYP2E1	PNP (100)	84 ± 4	136 ± 32	328 ± 30**	158 ± 28
CYP2D	AMMC (20)	70 ± 1**	102 ± 2	87 ± 2*,+	84 ± 3*,+
CYP3A	BQ (40)	78 ± 1***	104 ± 1	98 ± 1	95 ± 1

[1]The conditions used to measure the effects of particles on the rates of metabolism of probe substrates by different types of rat liver microsomes are specified in Materials and Methods. The values shown are the % relative rates of metabolism in the presence of 0.2 mg/ml of particles (silica with 5% copper oxide (CuO-Si), fumed silica, physisorbed MCP100, or physisorbed DCB100) and that of control reactions that contained equivalent amounts of saline and Tween 80.

[2]Rates are expressed as the average % rate (relative to the average rate of control incubations that contained no particles but had the same concentrations of saline and Tween 80) ± the standard error of three separate determinations. N.D. indicates activity not detected. Significantly different from the control reactions (*, $P < 0.05$; **, $P < 0.01$; ***, $P < 0.001$); significantly different the silica group ($^{+}$ $p < 0.05$; $^{+++}$ $p < 0.001$)